

UNCLASSIFIED

AD. 295 005

*Reproduced
by the*

**ARMED SERVICES TECHNICAL INFORMATION AGENCY
ARLINGTON HALL STATION
ARLINGTON 12, VIRGINIA**



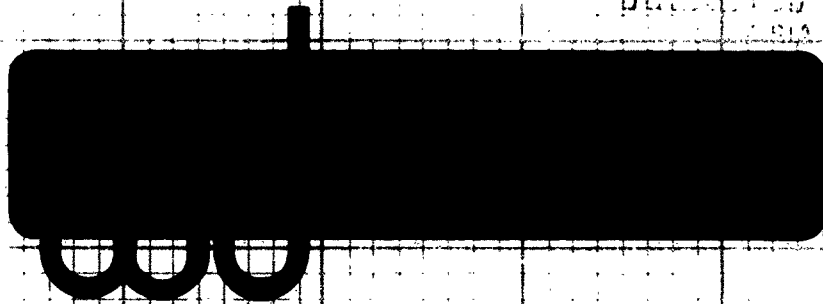
UNCLASSIFIED

NOTICE: When government or other drawings, specifications or other data are used for any purpose other than in connection with a definitely related government procurement operation, the U. S. Government thereby incurs no responsibility, nor any obligation whatsoever; and the fact that the Government may have formulated, furnished, or in any way supplied the said drawings, specifications, or other data is not to be regarded by implication or otherwise as in any manner licensing the holder or any other person or corporation, or conveying any rights or permission to manufacture, use or sell any patented invention that may in any way be related thereto.

CATALOGUE OF ASTIA
AS AD NO. 295005

295 005

63-6-3



ASTIA
JAN 28 1963

Interim Engineering Report No. 6
**APPLIED RESEARCH ON A
HIGH-POWER MILLIMETER-WAVE GENERATOR**

By
James W. Sedin

**Watkins-Johnson Company
3333 Hillview Avenue
Palo Alto, California**

1 September through 30 November 1962

**Contract Nr. AF 33(616)-8369
Task Nr 41533**

The applied research reported in this document has been made possible through support and sponsorship extended by the Electronic Technology Laboratory of the Aeronautical Systems Division, under Contract AF 33(616)-8369. It is published for technical information only and does not necessarily represent recommendations or conclusions of the sponsoring agency.

AERONAUTICAL SYSTEMS DIVISION

ABSTRACT

The purpose of this program is to demonstrate the feasibility of generating very high power, specifically, 100 kw peak and 1000 watts average at 100 Gc by means of an O-type backward-wave oscillator operating at very high voltage.

During the sixth quarter, the new electron gun, designated gun No. 435-1B, was completely tested and evolved and a final design model has been constructed for experimental tube No. 2. Calculated and measured data for this gun design is presented. Further work has been done on silicon carbide loaded glaze for use as a high power waveguide attenuator. A suitable design has been evolved and loads are being constructed. Minor difficulties have been encountered in electroforming the circuits. A fixture for holding the waveguide and circuit mandrels in the proper orientation has been constructed. Experimental tube No. 2 is in the final stages of assembly.

A discussion of the difficulties encountered in attempting to use existing nonrelativistic gun calculations for relativistic cases is presented.

TABLE OF CONTENTS

	<u>Page No.</u>
INTRODUCTION	1
ELECTRON GUN NO. 435-1B	1
WAVEGUIDE LOADS	3
TUBE CONSTRUCTION	17
CONCLUSIONS	17
REFERENCES	19
APPENDIX - BEAM DIAMETER INCLUDING THERMAL EFFECTS UNDER RELATIVISTIC VELOCITY CONDITIONS	20
The Drift Region	22
The Anode Lens	23
The Gun Region	26
The Complete Problem	26

LIST OF ILLUSTRATIONS

<u>Figure No.</u>		<u>Page No.</u>
1	Pertinent gun dimensions for gun No. 9 which was used in experimental tube No. 1 and gun No. 435-1B which is being used in tube No. 2.	2
2	Gun 435-1 dimensions as tested in demountable beam analyzer.	4
3	Beam current profiles at the beam minimum for gun 435-1 at 2 kv and 4 kv beam voltage.	5
4	Beam diameter as a function of beam voltage for gun 435-1.	6
5	Diameter enclosing 95 percent of the beam current plotted as a function of beam voltage for gun No. 9 which was used in tube No. 1 and for gun 435-1B which is being used in tube No. 2.	8
6	Anode-cathode assembly of gun 435-1B as it is being used in tube No. 2.	9
7	Drawing of experimental tube No. 1.	10
8	Drawing of experimental tube No. 2.	11
9	High power waveguide attenuator made as described in the text.	14
10	Waveguide loads for the collector end of the circuit.	15
11	Aluminum waveguide and circuit mandrels in a phenolic frame prior to final electroforming.	16
12	Completed 435-1B gun assembly prior to mounting on the anode.	18

INTRODUCTION

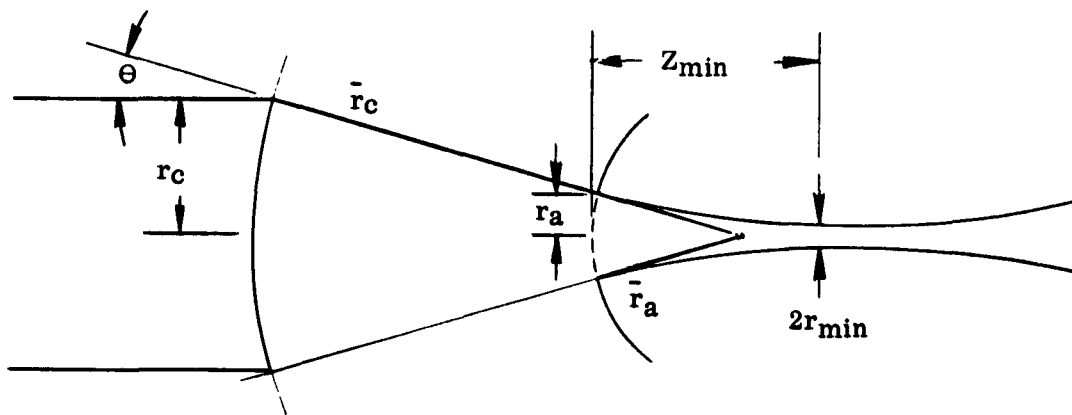
The purpose of this program is to demonstrate the feasibility of generating very high power, specifically, 100 kw peak and 1000 watts average at 100 Gc by means of an O-type backward-wave oscillator operating at very high voltage.

During the sixth quarter, the new electron gun, designated gun No. 435-1B, was completely tested and evolved and a final design model has been constructed for experimental tube No. 2. Calculated and measured data for this gun design is presented. Further work has been done on silicon carbide loaded glaze for use as a high power waveguide attenuator. A suitable design has been evolved and loads are being constructed. Minor difficulties have been encountered in electroforming the circuits. A fixture for holding the waveguide and circuit mandrels in the proper orientation has been constructed. Experimental tube No. 2 is in the final stages of assembly.

ELECTRON GUN NO. 435-1B

The difficulties that were experienced in focusing the beam in tube No. 1 led to the design of a new electron gun as described briefly in the preceding quarterly report. During the past quarter this gun, designated 435-1B, has been tested in the demountable beam tester and modified slightly to yield a desirable mechanical configuration. Fig. 1 summarizes the design characteristics of gun No. 435-1B in comparison to gun No. 9 which was used in experimental tube No. 1. The perveance of gun 435-1B is approximately $.125 \times 10^{-6}$, almost identical to the perveance of gun No. 9. The important differences between the two guns are:

1. The cathode radius has been reduced from .6 inch to 0.45 inch thus increasing the peak cathode loading at 11 amperes beam current from 1.6 a/cm^2 to 2.8 a/cm^2 .
2. The beam diameter at the minimum has been increased from an estimated 7.5 mils diameter to an estimated 44 mils diameter at 200 kv. As a result, beam scalloping should be greatly reduced because the beam will enter the magnetic field at approximately the desired diameter. In addition, rf interaction will be stronger because the beam diameter will be larger where the rf fields are strongest.



	<u>Gun No. 9</u>	<u>Gun No. 435-1B</u>
$\frac{\bar{r}_c}{\bar{r}_a}$	5.24	2.636
\bar{r}_c	1.755 inches	2.59 inches
\bar{r}_a	.334 inch	.985 inch
r_c	0.6 inch	0.45 inch
r_a	.114 inch	.171 inch
θ	20°	10°
Z_{min}	.62 inch measured at 4 kv	1.84 inches (measured at 4 kv)
$(2r_{min})_{95\%}$.0075 inch (computed at 200 kv)	.044 inch (computed at 200 kv)
perveance	$.125 \times 10^{-6}$	$.125 \times 10^{-5}$

Fig. 1 - Pertinent gun dimensions for gun No. 9 which was used in experimental tube No. 1 and gun No. 435-1B which is being used in tube No. 2.

3. The beam minimum has moved further away from the cathode. The distance from the anode to the minimum has increased from 0.62 inches to 1.84 inches as measured at 4 kv. As a result, the magnetic pole piece on the gun end of the circuit can be made re-entrant and the leakage magnetic fields will be greatly reduced.

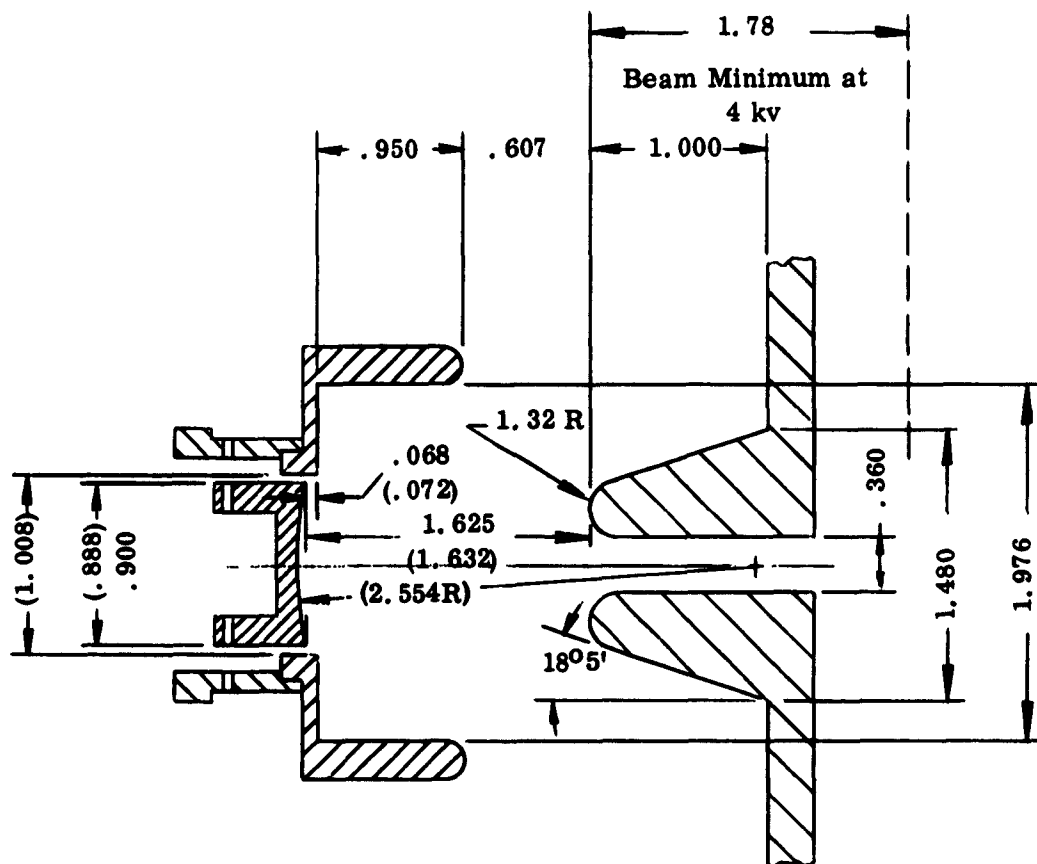
Fig. 2 is a drawing which shows the actual focus electrode and anode shapes used in gun 435-1 as tested in the demountable beam tester. Fig. 3 shows measured beam current density profiles at 2 kv and 4 kv beam voltage. Fig. 4 is a plot of beam diameter as a function of beam voltage at low voltages. The measured 99 percent current diameters were estimated from current density measurements as shown in Fig. 3. Agreement is quite good in view of the rough method used for determining 99 percent beam current. Table I summarizes the calculations using the results of Danielson, Rosenfeld, and Saloom¹ as generalized by Herrmann². The values for voltages greater than about 25 kv are very approximate for two reasons. One reason is that the calculations of Danielson et al. do not extend to the range of parameters encountered and the curves were extrapolated. The second reason is that when relativistic effects become important, the scaling rules do not necessarily apply. A discussion of the approximations used in determining an effective value of $\frac{pV}{T}$ is given

in the Appendix. Fig. 5 is a plot of calculated beam diameter as a function of beam voltage for gun No. 9 which was used in experimental tube No. 1 and gun No. 435-1B which will be used in experimental tube No. 2.

Fig. 6 is a drawing of the complete cathode-anode assembly of gun 435-1B as it is being used in experimental tube No. 2. The diameter of the anode hole is only 0.060 inch so it will be impossible to obtain 100 percent beam transmission for voltages less than about 50 or 60 kv since the beam diameter is greater than 0.060 inch. A copper insert is being used inside the iron anode to prevent overheating of the surfaces during the rise and fall of the voltage pulse.

WAVEGUIDE LOADS

Fig. 7 is a drawing of experimental tube No. 1. Fig. 8 is a similar drawing of tube No. 2 which is presently under construction. The only external differences are the tapered anode pole piece which is a result of the modified gun design described above and the change in the output waveguides. Experimental tube No. 1 had a 40 db single-hole coupler for sampling the power and a 0.2 liter ion pump after the high power load on each arm. Experimental tube No. 2 will have only a high power load with a compression seal mica window on each waveguide arm.



Dimensions in brackets
cold, all others hot

Fig. 2 - Gun 435-1 dimensions as tested in demountable beam analyzer. Gun 435-1B is identical to gun 435-1 with the exception of the focus electrode and anode geometry. 435-1B was modified slightly to simplify the construction without changing the beam edge potential.

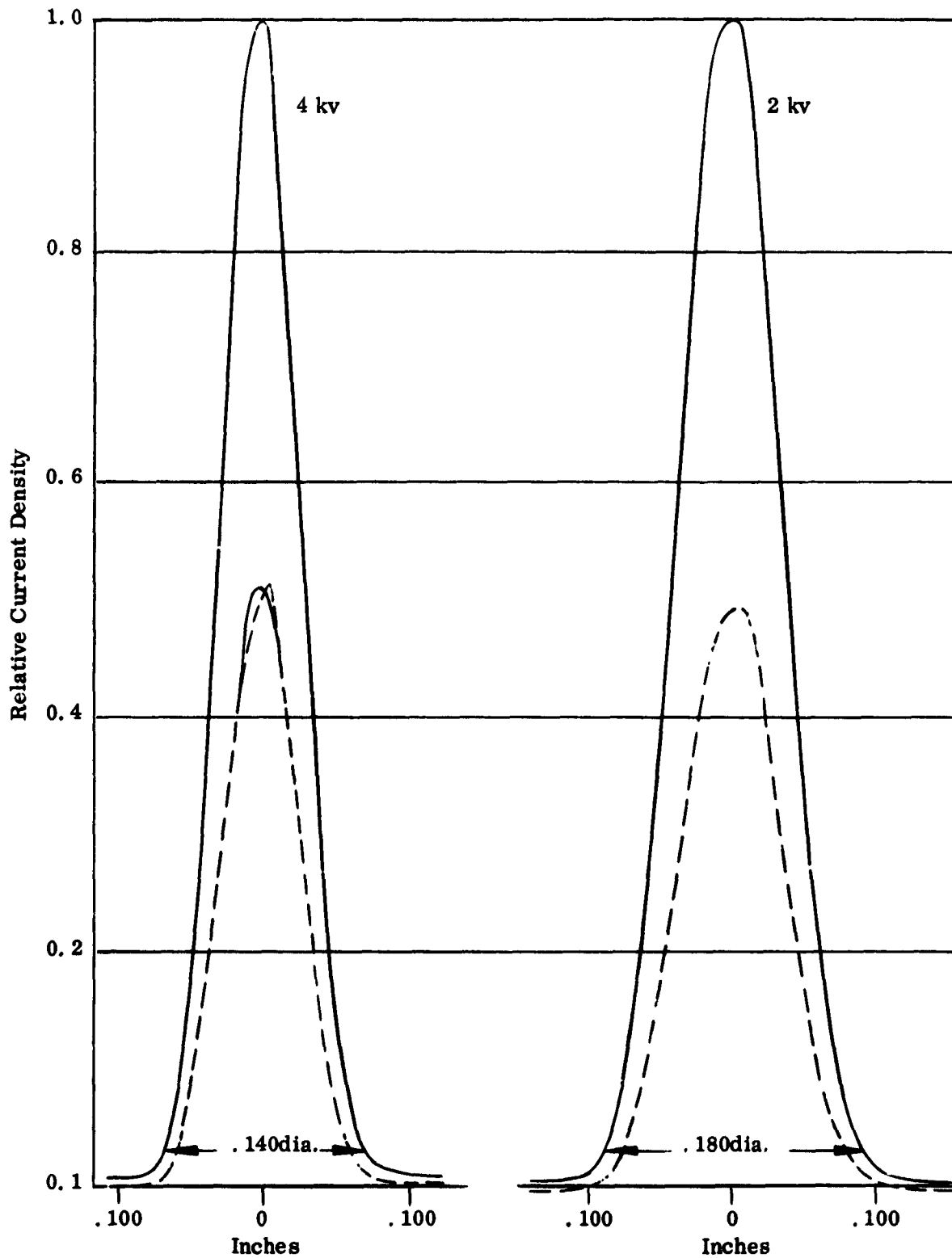


Fig. 3 - Beam current profiles at the beam minimum for gun 435-1 at 2kv and 4kv beam voltage. The dashed line should actually be a double line which shows the amount of current on each half of a split collector. The currents on the two halves are virtually identical, indicating that gun aberrations are small.

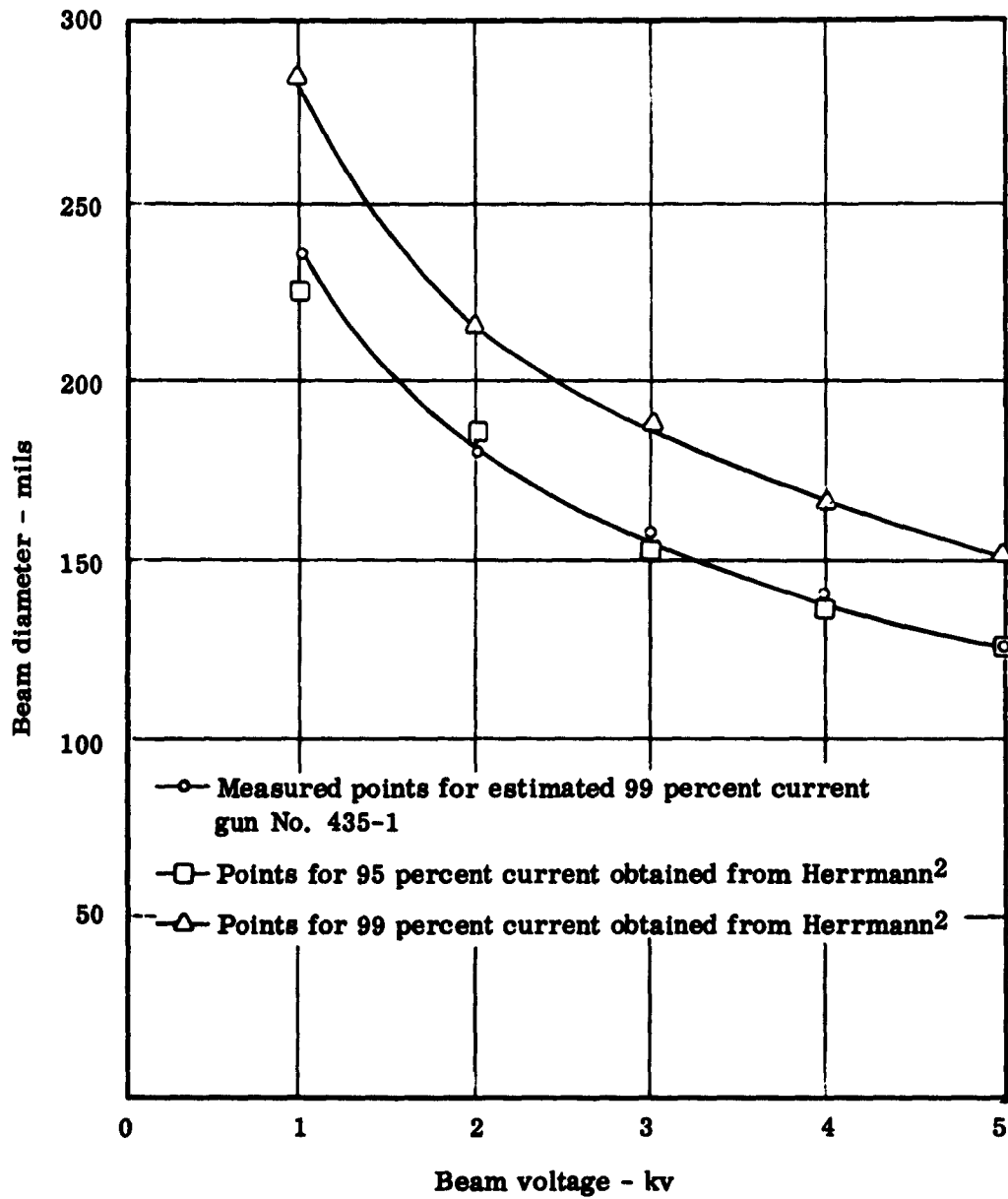


Fig. 4 - Beam diameter as a function of beam voltage for gun 435-1. The agreement between calculated and measured diameters is good. The 99 percent current points were only estimated from the measured beam profiles.

TABLE 1

V(kv)	Gun No. 9					Gun 435-1B				
	$\frac{pI^*}{T} \times 10^{-6}$	$\frac{r_{min}}{\bar{r}_c} 95\%$	$\frac{Z_{min}}{\bar{r}_c}$	$\frac{Z_{min}}{\bar{r}_c}$ (measured)	$\frac{r_{min}}{\bar{r}_c} 95\%$	$\frac{Z_{min}}{\bar{r}_c}$	$\frac{Z_{min}}{\bar{r}_c}$ (measured)	$\frac{r_{min}}{\bar{r}_c} 95\%$	$\frac{Z_{min}}{\bar{r}_c}$ (measured)	$\frac{r_{min}}{\bar{r}_c} 99\%$
1	.114	.08			.25			.65		.317
2	.227	.06	.4		.19					.24
3	.341	.05			.17					.21
4	.455	.04	.4	.35	.15			.75	0.7	.185
5	.569	.038			.14			.83		.17
14	1.6	.023	.4		.1					
25	2.84	.018			.085			.85		
50	5.55	.011	.4		.07			.9		
100	10.8	.009			.06			.93		
200	19.9	.006	.4		.049			.96		

* A cathode temperature of 1100° K has been assumed. At extremely high voltages, an effective $\frac{pV}{T}$ has been used as described in the Appendix.

Calculated and measured characteristics of gun No. 9 and gun No. 435-1B

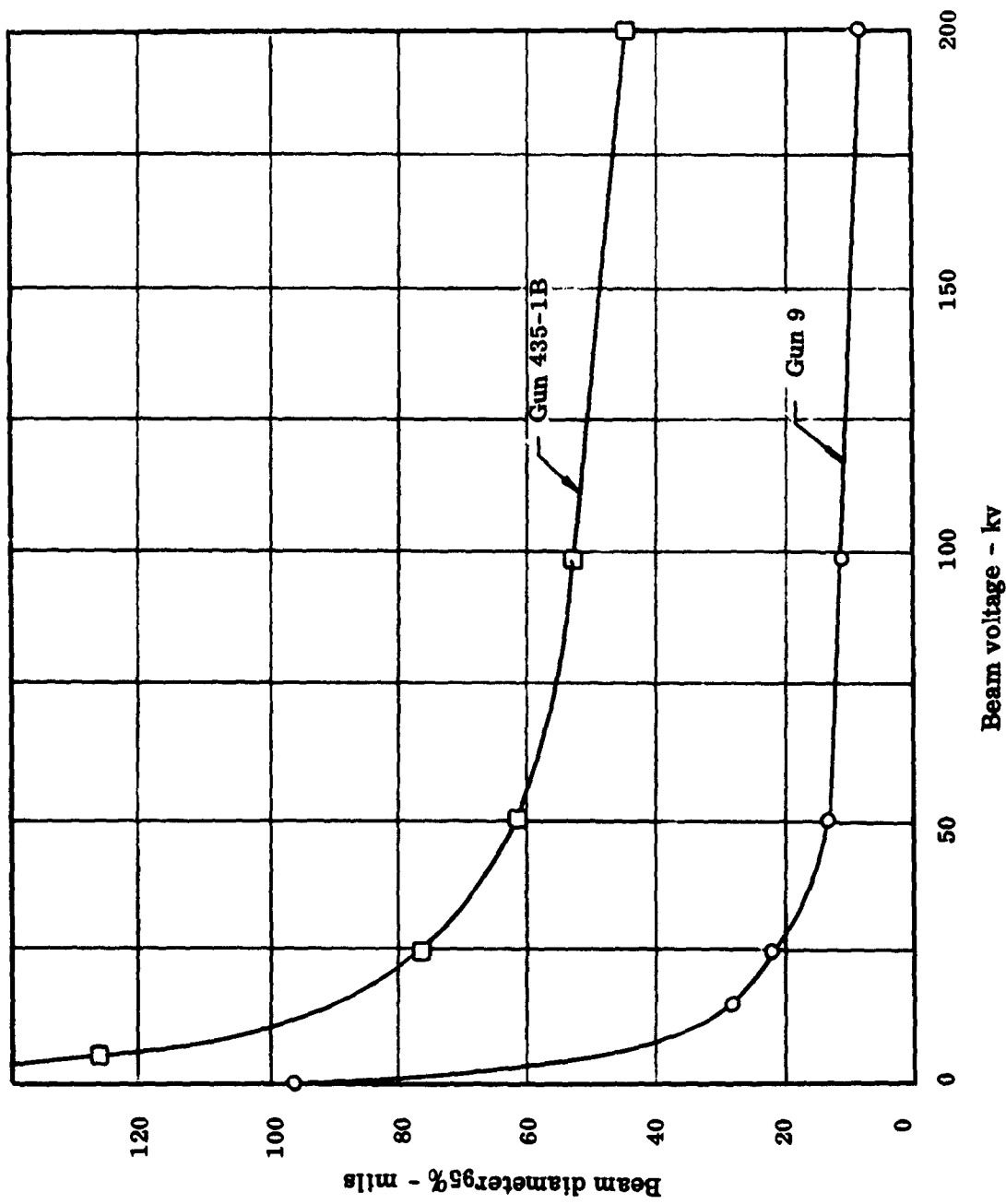


Fig. 5 - Diameter enclosing 95 percent of the beam current plotted as a function of beam voltage for gun No. 9 which was used in tube No. 1 and for gun 435-1B which is being used in tube No. 2. These curves were obtained from the results of Danielson, Rosenfeld, and Saloom¹ as generalized by Herrmann². The calculated data is given in Table 1. The pertinent gun dimensions are given in Fig. 1.

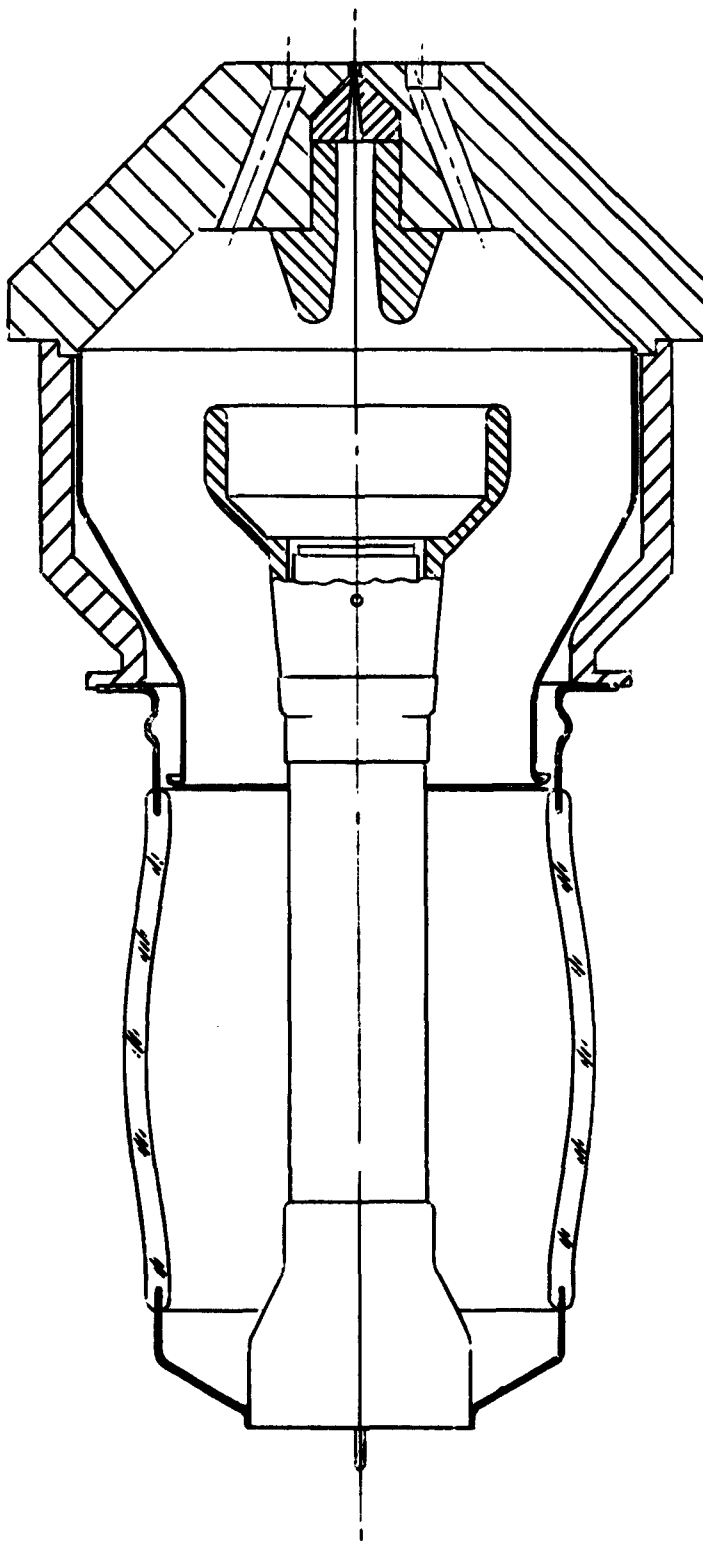


Fig. 6 - Anode-cathode assembly of gun 435-1B as it is being used in tube No. 2. The only differences between this gun and the gun shown in Fig. 2 are that the focus electrode has a 45° angle on the inside corner and the anode wall has been moved closer to the anode tips.

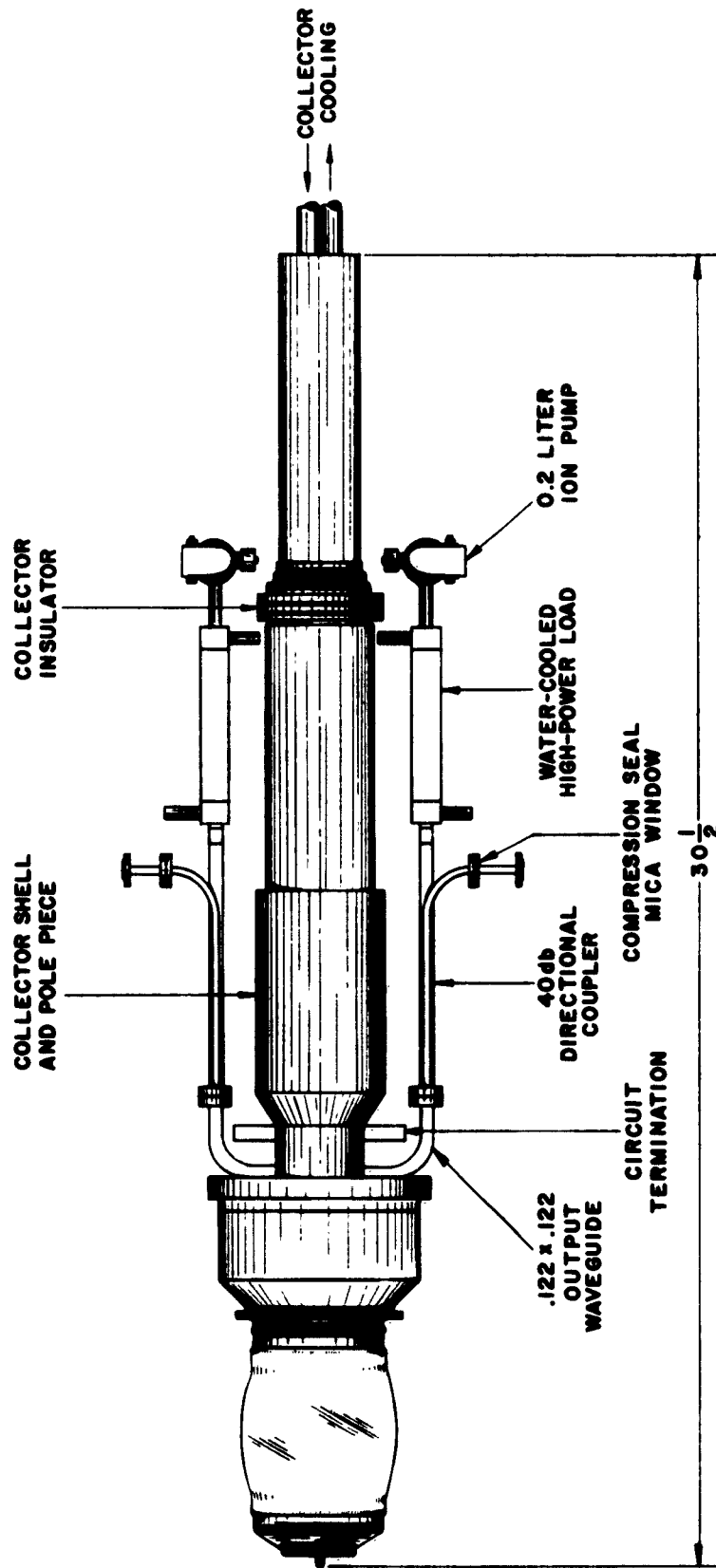


Fig. 7 - Drawing of experimental tube No. 1.

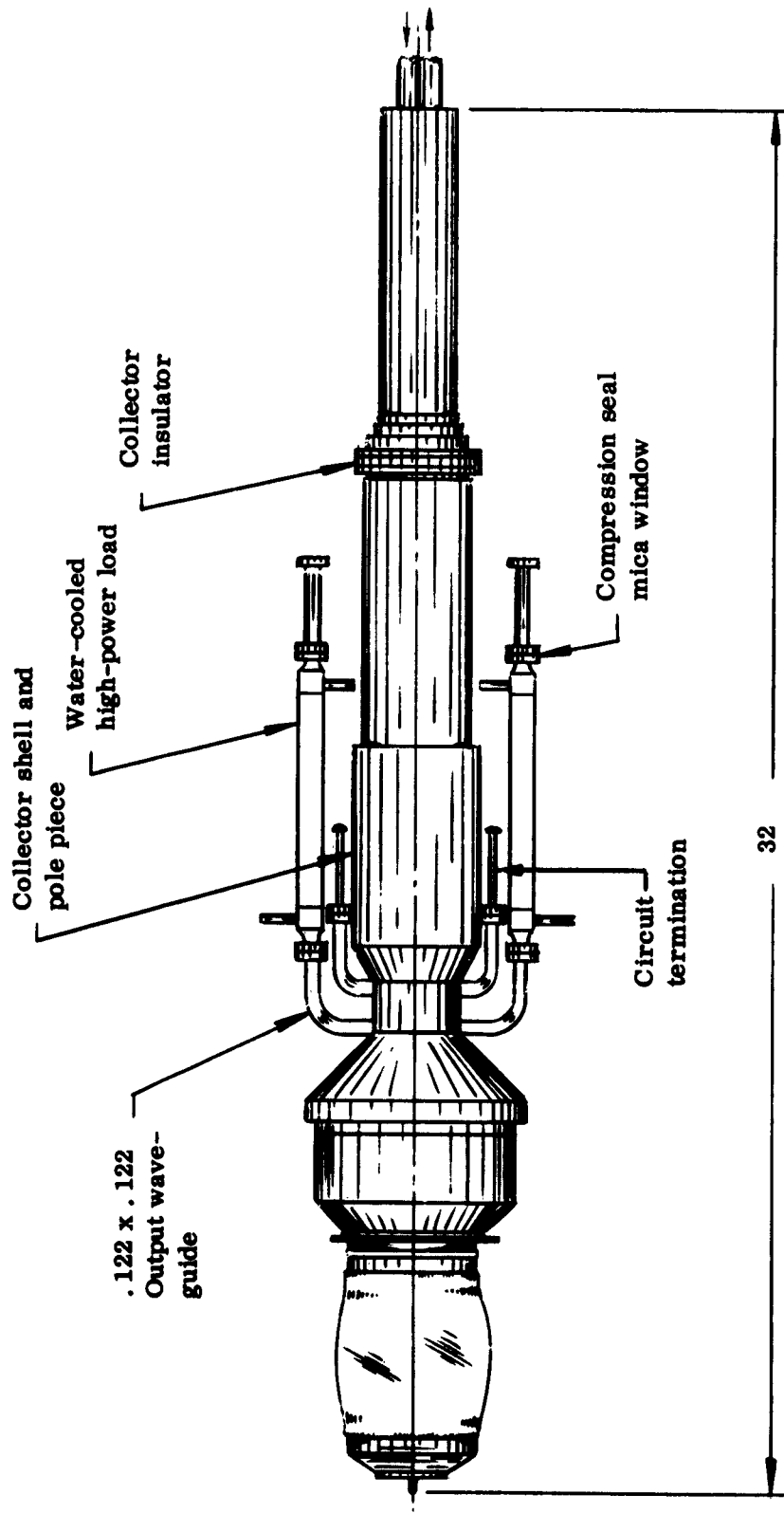


Fig. 8 - Drawing of experimental tube No. 2. The only external changes are in the anode pole piece and the elimination of the 40 db coupler and 0.2 liter ion pump.

The change from the 40 db coupler to a straight through high power load has been made in an effort to increase the accuracy of the rf power measurements. The accuracy of the power measurements in tube No. 1 was poor because the actual coupling through the nominal 40 db coupler varied rapidly as a function of frequency. This variation was mainly due to reflections from the high power load. Reasonably accurate rf power measurements could only be made at almost exactly the frequency for which coupler calibration points existed.

The high power loads used on tube No. 1 were constructed by electroforming copper over a rough stainless steel surface to form a copper waveguide lined with sprayed stainless steel. The copper formed in this way was porous and the complete load assembly was not particularly satisfactory. The high power loads for experimental tube No. 2 are being made by coating the inside of a molybdenum waveguide with a lossy glaze material. The lossy glaze consists of 85 percent silicon carbide, 325 mesh particle size, and 15 percent Bell Telephone Laboratories glaze M-24. The BTL M-24 glaze consists of -

Li CO ₃	13 percent by weight
Ca CO ₃	8.9 percent
BaCO ₃	17.9 percent
Al ₂ O ₃	18 percent
SiO ₂	42.2 percent

The particle size is 4-35 microns. The BTL glaze mixture is purchased from Thomas C. Thompson and Co., Highland Park, Illinois. The silicon carbide and M-24 glaze is mixed with a touch of pyroxylin as a binder and amyl acetate as a thinner. It is thinned to appropriate brushing consistency. The lossy glaze mixture is then fired onto the molybdenum waveguide at 1210°C in wet hydrogen for 30 minutes. Molybdenum waveguide is used because silicon carbide has a very low coefficient of thermal expansion, even lower than molybdenum. BTL M-24 glaze is a low expansion glaze suitable for bonding molybdenum to ceramic.

The amount of loss obtained can be varied by varying the thickness of the coating, the fraction of the perimeter of the waveguide wall covered, and the total length of load. Applying the loss is a cut-and-try procedure. The waveguides presently being used are 0.122 x 0.122 inch inside dimensions. They are made in the form of a channel with a separate cover. The glaze is painted and fired onto the waveguide surfaces. The cover is then clamped in place and the loss measured. Additional loss can then be added if necessary by repeating the procedure.

Fig. 9 is a photograph of a load made in the manner just described. The overall length of the load is 4.5 inches and the loss is about 30 db. The loss was applied to 3 walls of the guide. The loss material is 10-12 mils thick at the thickest place. We are not planning to use this particular load on experimental tube No. 2. We are planning to increase the total length of the load to 7 inches and put loss on all four waveguide walls so that about 25-30 db of loss can be obtained with a very thin coating of lossy material. The reduction in coating thickness and increase in total area will reduce the thermal gradients that will occur at high power levels, thus minimizing the possibility of the glaze flaking off of the molybdenum walls.

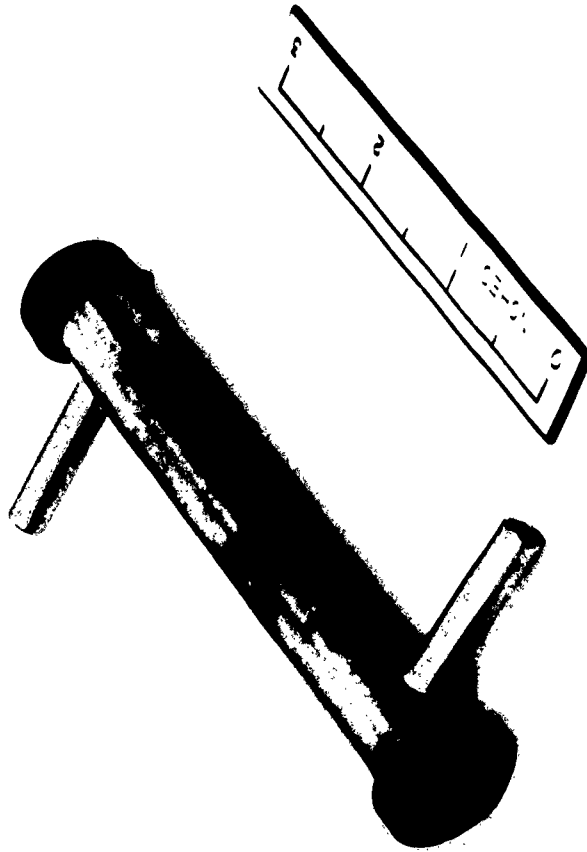
Fig. 10 is a photograph of the glazed loads that will be used to terminate the collector end of the circuit. These loads are also 0.122 x 0.122 inch square molybdenum guide. These loads are only 2.2 inches long and do not have an integral water jacket because they will be required to dissipate only 10-20 percent as much power as the output loads.

CIRCUIT CONSTRUCTION

The procedure for constructing the circuits by electroforming was described in the Third Interim Engineering Report. The only modification that has been made in this procedure is to hold the aluminum circuit and waveguide mandrels in a paper-based phenolic frame as shown in Fig. 11. The purpose of this frame is to maintain waveguides accurately perpendicular to the circuit mandrel and firmly seated in the notches in the circuit mandrel. Several circuits have previously been lost because the waveguides did not remain properly seated in the circuit mandrel.

The circuits are carefully inspected at each end with a microscope. It is possible to see the matching posts through the beam hole at each end. It is also possible to see if the waveguides are properly joined to the circuit. The copper is inspected after it has been hydrogen fired at 950°C. Visual inspection of the circuits is sufficient to detect any gross inaccuracies in the circuit. Further inaccuracies can only be detected by analysis of the electrical performances.

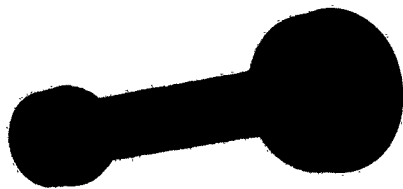
At the present time, one complete circuit assembly is brazed into a copper circuit block. Three circuit mandrels are in the process of receiving the initial copper layer prior to remachining the grooves. The electroforming is being done by Physical Electronics Laboratories, East Palo Alto, California. Some circuits have been electroformed at Watkins-Johnson Company. However, since insufficient electroforming is done at Watkins-Johnson Company to require full time use of an electroforming bath, it is felt that the control of the quality of copper is probably better from Physical Electronics Laboratories where the tanks are in continuous use.



WATSON
W

Fig. 9 - High power waveguide attenuator made as described in the text.

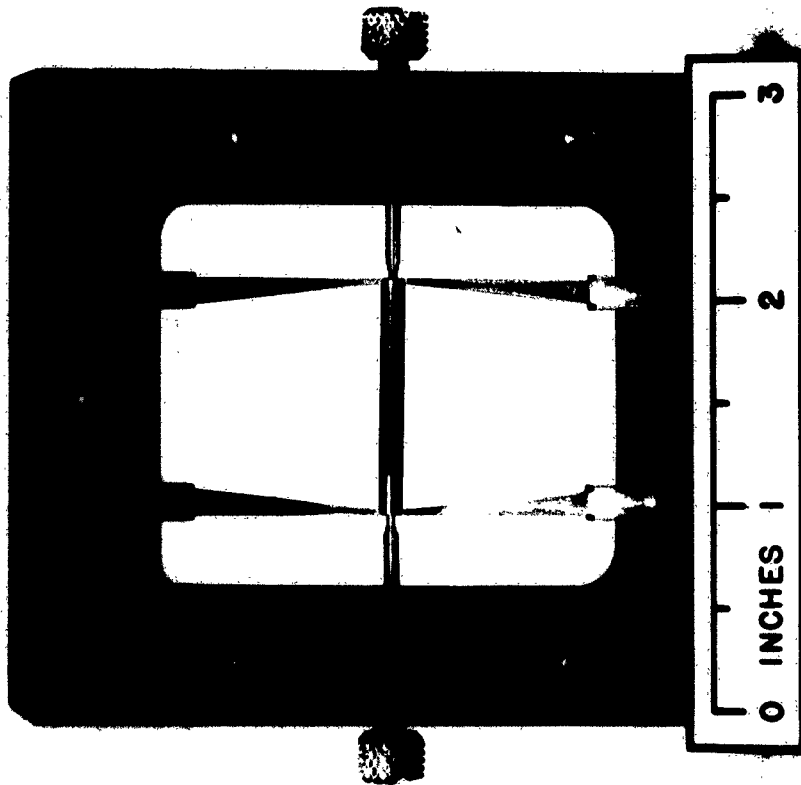
2807-6



33

Fig. 10 - Waveguide loads for the collector end of the circuit. These loads are made in the same way as the high power loads except that they do not have an integral water cooling jacket.

2007-5



WATSON JENSEN

Fig. 11- Aluminum waveguide and circuit mandrels in a phenolic frame prior to final electroforming. The frame holds the waveguides securely in position.

2887-3

TUBE CONSTRUCTION

Experimental tube No. 2 is in the final stages of assembly. Fig. 12 is a photograph of the completed gun assembly for gun 435-1B. A collector assembly identical to the one used on tube No. 1 has been completed. The anode and collector pole pieces, and waveguide arms have not yet been brazed to the circuit assembly. A new set of output loads is being constructed as described above. Tube No. 2 will be completed during the next report period.

CONCLUSIONS

No conclusions can be drawn as a result of the work completed during the past quarter.



Fig. 12 - Completed 435-1B gun assembly prior to mounting on the anode.

REFERENCES

1. W. E. Danielson, J. L. Rosenfeld, J. A. Saloom "Analysis of Beam Formation with Electron Guns of the Pierce Type", BSTJ Vol. 35 pp 375-420, March 1956.
2. G. B. Herrmann, "Optical Theory of Thermal Velocity Effects In Cylindrical Beams", Jour. Appl. Phys. , Vol. 19, No. 2, pp. 127 to 136; February 1958.

APPENDIX

Beam Diameter Including Thermal Effects Under Relativistic Velocity Conditions

The analysis of beam formation in Pierce type electron guns carried out by Danielson, Rosenfeld, and Saloom⁽¹⁾ in which the effects of thermal velocities are large compared to space charge effects has given results in good agreement with experimental results for low voltage operation. These results are not directly applicable to situations in which the electrons reach relativistic velocities since the equations of motion are more complicated under relativistic conditions. The following discussion describes an approximate procedure for utilizing the results under relativistic velocity conditions.

Briefly, the procedure used by Danielson, Rosenfeld, and Saloom is to divide the beam forming region into three (3) parts, the cathode-anode region, the anode lens, and the field free drift region between the anode lens and the beam minimum. Thermal velocity effects are included in the cathode-anode region by considering the motion of an electron emitted from the center of the cathode with a finite transverse velocity. It is shown that the transverse position of an electron at any axial position is proportional to the transverse velocity at the cathode. It is therefore possible to compute the transverse distribution in space at any axial position of electrons emitted from the center of the cathode with different transverse velocities from a knowledge of the transverse velocity distribution at the cathode. It is only necessary to calculate the motion of a single electron emitted with some transverse velocity (chosen to be $\sqrt{\frac{kT}{m}}$) from the center of the cathode and the motion of an electron emitted from the edge of the cathode with zero transverse velocity. These electrons are called the σ and r_e electrons respectively and σ and r_e are the radial positions of these electrons at any point in the gun region. If the paths of the thermal electrons do not deviate greatly from the paths of the non-thermal electrons, the space charge forces on the electrons can be considered to be the same as the space charge forces in the absence of thermal effects. Since the cathode-anode region of a Pierce gun is a section of a sphere, electrons emitted with finite transverse velocities from any point on the cathode will distribute about an electron emitted from the same point with zero transverse velocity in exactly the same way as they do about the electron emitted from the center of the cathode with zero transverse velocity (neglecting effects at the edge of the beam). The current density as a function of radius can thus be computed in the cathode-anode region if the transverse motion due to thermal effects is small compared to the ideal beam diameter in the absence of thermal effects. This is true in a large number of electron guns.

At the anode lens, the diverging effect of the lens is applied to the trajectories of the σ and r_e electrons.

In the field free region between the anode lens and the beam minimum σ becomes comparable to or greater than r_e in many electron guns and the assumption that the electrons move in space charge fields equal to those that would occur in the absence of thermal effects is not valid. Danielson, Rosenfeld, and Saloom assume that the r_e and σ electrons move in space charge fields from a beam in which thermal electrons are distributed about non-thermal electrons in a Gaussian manner with standard deviation σ . The current density of non-thermal electrons is assumed to be constant for $r < r_e$. The solutions for σ and r_e are therefore interdependent and must be solved simultaneously using computer techniques. The results obtained are in good agreement with experimental results.

In order to carry out the analysis just described under relativistic conditions it would be necessary to substitute the relativistic equations in each of the three regions. The analysis would become very complicated. Fortunately, in the drift region where the beam shape deviates considerably from the ideal shape, the equations of motion can be used in exact form. At the anode lens it is possible to obtain an estimate of the relativistic effects on the lens divergence. In the cathode-anode region the problem is complicated and some rather qualitative arguments will be used to justify the effective gun parameters.

Herrmann² has shown that in a number of practical situations it is possible to subject a beam to a process of scaling in which the transverse components of position, velocity, and force are scaled by a common factor while longitudinal components remain unchanged. The application of transverse scaling simplifies the treatment of guns under thermal velocity conditions by allowing a reduction in the number of independent variables required. He was thus able to present the data calculated by Danielson, Rosenfeld, and Saloom in a form in which is applicable to a much wider variety of cases. If the simple Davission electrostatic lens formula is used with a constant correction factor for the anode lens, Danielson, et al. presented the computed data in terms of three parameters, the ratio of the cathode radius to the anode radius

$\frac{\bar{r}_c}{\bar{r}_a}$, the perveance p , and the ratio of the anode voltage to the cathode temperature

$\frac{V_{\text{anode}}}{T_{\text{cathode}}}$. Herrmann presented the data in terms of $\frac{\bar{r}_c}{\bar{r}_a}$ and $\frac{pV_a}{T}$.

In order to make use of the calculated results at relativistic velocities it is necessary to define an effective value of $\frac{pV_a}{T}$. A method for selecting this value is presented here.

The Drift Region

In the drift region the only forces acting on the electrons are the space charge forces and the forces due to the magnetic field of the beam. If the beam is approximately cylindrical there are only radial forces and the equation of motion is:

$$m_t \frac{d^2 r}{dt^2} = \frac{e}{2\pi \epsilon_0 r} \frac{I_r}{v} - \frac{e \mu_0 v I_r}{2\pi r} \quad 1A$$

where $m_t = \frac{m_0}{\sqrt{1 - \frac{v^2}{c^2}}}$ is the transverse mass of the electron I_r is the

current contained within the radius r

v = the electron velocity

e = the magnitude of the electronic charge

Equation 1A can be written:

$$\frac{d^2 r}{dt^2} = \frac{I_r e}{2\pi \epsilon_0 r m_0 v} \left[1 - \frac{v^2}{c^2} \right]^{3/2} \quad 2A$$

The velocity in the z direction is approximately constant and equal to v

$$\frac{d^2 r}{dz^2} = \frac{I_r e}{2\pi \epsilon_0 m_0 r} \frac{\left[1 - \frac{v^2}{c^2} \right]^{3/2}}{v^3} \quad 3A$$

This equation is identical to that which would be obtained in the absence of space effects with the exception of the term $\left[1 - \frac{v^2}{c^2} \right]^{3/2}$ If an equivalent velocity

$$v_{eq} = \frac{v}{\sqrt{1 - \frac{v^2}{c^2}}} \quad 4A$$

an equivalent voltage

$$V_{eq} = \frac{m_0 V_{eq}^2}{2e} \quad 5A$$

and an equivalent perveance

$$P_{eq} = \frac{I_0}{V_{eq}^{3/2}} \quad 6A$$

are defined,

$$\frac{d^2r}{dz^2} = \frac{1}{4\pi\epsilon_0\sqrt{z\eta}} \frac{I_0}{V_{eq}^{3/2}} \quad \frac{F}{r} = \frac{P_{eq}}{4\pi\epsilon_0\sqrt{2\eta}} \frac{F}{r} \quad 7A$$

where $F = \frac{I_r}{I_0}$ is the fraction of the total current contained within

radius r .

Equation 7A is exactly the equation for the trajectory of an electron in a long beam under space charge forces under non-relativistic conditions. The relativistic effects are accounted for by the definition of an equivalent voltage and perveance as described above. The universal beam spread curve as given by Spangenberg⁽³⁾ for example can be used under relativistic conditions if the equivalent perveance defined by Eqs. 4A, 5A, and 6A is used. The treatment of the drift region by Danielson et al. would also be correct if the equivalent perveance is used. However, the boundary conditions on r_e , $\frac{dr_e}{dz}$, σ , and $\frac{d\sigma}{dz}$ at the beginning of the drift

region would not necessarily be correct since the force equation in the cathode-anode region can not be modified in such a simple manner.

The Anode Lens

Danielson et al. described a method for determining the focal length of the anode lens more accurately than is given by the Davisson focal length. The Davisson focal length is

$$F_D = -\frac{4V}{dV/dz}$$

where $\frac{dV}{dz}$ is the magnitude of the electric field at the anode aperture if it

were gridded and V is the voltage there. The results of the more exact analysis of the anode lens led Danielson et al. to modify the focal length to

$$F = \frac{F_D}{\Gamma}$$

where Γ is a correction factor. They found Γ to be typically of the order of 1.1 and most of their calculations were carried out for $\Gamma = 1.1$.

The Davisson method for determining the focal length could be used under relativistic conditions. However, it would require a solution to the problem of space charge limited current flow in a spherical diode under relativistic conditions.

The equation for radial motion of an electron in the absence of Θ components of velocity (in cylindrical coordinates) is

$$m_t \frac{d^2 r}{dt^2} = e \frac{\partial V}{\partial r} \quad 8A$$

where again

$$m_t = \frac{m_0}{\sqrt{1 - \frac{v^2}{c^2}}}$$

By expanding the potential in power series about the axis and neglecting higher order terms

$$V(z, r) = V - \frac{1}{4} \frac{d^2 V}{dz^2} r^2 \quad 9A$$

$$\frac{\partial V}{\partial r} = -\frac{1}{2} \frac{d^2 V}{dz^2} r \quad 10A$$

In the vicinity of the anode lens, the axial electron velocity is approximately constant, $\frac{dz}{dt} = v$ and the radial position r is approximately constant.

$$\frac{d^2 r}{dz^2} = -\frac{e}{2m_t v^2} \frac{d^2 V}{dz^2} r \quad 11A$$

Integrate once

$$\frac{dr}{dz} /_2 - \frac{dr}{dz} /_1 = -\frac{er}{2m_t v^2} \left(\frac{dV}{dz} /_2 - \frac{dV}{dz} /_1 \right) \quad 12A$$

where $\frac{dr}{dz} /_2$ is the slope of the trajectory after passing through the lens and $\frac{dr}{dz} /_1$ is the slope before the lens. Since the region after the lens is field free, $\frac{dV}{dz} /_2 = 0$.

The focal length of the lens then is

$$F = - \frac{2m_t v^2}{e} \frac{1}{\frac{dV}{dz}}$$

Under nonrelativistic conditions,

$$\frac{mv^2}{2e} = V$$

and
$$F = - \frac{4V}{\frac{dV}{dz}}$$

which is the Davisson focal length.

Under relativistic conditions,

$$\frac{1}{F} = \left(\frac{2Ve}{m_t v^2} \right) \frac{dV}{dz} \quad F = - \left(\frac{m_t v^2}{2Ve} \right) \frac{4V}{dz}$$

where the term in brackets is a correction to the nonrelativistic focal length. In addition the value of $\frac{dV}{dz}$ is slightly different from the value under nonrelativistic conditions.

As an example, at 200 kv $\frac{v}{c} \approx 0.7$
and the correction factor is

$$\frac{m_0 c^2}{2Ve} \times \frac{0.7^2}{\sqrt{1-0.7^2}} = \frac{511}{2 \times 200} \times \frac{.5}{.7} = .915$$

Under relativistic conditions, $V/\frac{dV}{dz}$ at the anode in a spherical diode is not really the same as it is under nonrelativistic conditions. Since the electrons are actually going slower, there is a sort of piling up of charge near the anode which would increase $\frac{dV}{dz}$ and actually reduce the gun perveance slightly. The increase in $\frac{dV}{dz}$ would further decrease the focal length over the nonrelativistic focal length. This means that the anode lens is somewhat more diverging under relativistic conditions that it is under nonrelativistic conditions. Although the effective transverse mass of the electrons is greater, the electrons actually are deflected more because they are traveling more slowly in the vicinity of the lens than they would if the velocity were proportional to \sqrt{V} .

The minimum beam diameter obtained from the computations of Danielson et al. can therefore be expected to be somewhat smaller than the beam diameter that will actually be obtained under relativistic conditions. The over-all effect of the corrections to the focal length are relatively small, probably less than 10 percent so it is unlikely that any gross errors will be introduced by neglecting the relativistic correction to the focal length.

The Gun Region

The gun region is the most difficult region to treat exactly under relativistic conditions since the electron velocity varies over extreme ranges in the gun region. Fortunately, in the gun region of most typical electron guns, the beam shape with thermal effects included does not deviate greatly from the beam shape in the absence of thermal effects. The specification of $\frac{r_c}{r_a}$ and the perveance actually specifies the convergence angle of an ideal spherical gun and in turn $\frac{r_e}{r_c}$, the position of a nonthermal edge electron in terms of the actual cathode radius. The position σ_a of the typical thermal electron at the anode is proportional to $\sqrt{\frac{T}{V_a}}$ for a given gun. This is reasonable since the transverse velocities of emission are proportional to \sqrt{T} and the time required to transverse the anode-cathode space is inversely proportional to the velocity of the electrons.

Under relativistic conditions, the transverse velocities are decreased because the transverse mass of the electrons increases as $\frac{m_0}{\sqrt{1 - v^2/c^2}}$. However, the time required

to transverse the cathode anode space is greater than it would be if the velocity were proportional to \sqrt{V} so the values of σ_a and $\frac{d\sigma}{dz}_a$ and the anode are probably greater

than they would be if relativistic effects were not included in the calculation. The calculations for the anode lens indicated a decrease of about 10 percent in the focal length of the lens at 200 kv. The increase in $\frac{d\sigma}{dz}_a$ at the anode is probably less than

10 percent since relativistic effects are only significant for a relatively small fraction of the time spent in traversing the cathode-anode region.

The Complete Problem

In order to use the results of Danielson et al. as generalized by Herrmann, it is necessary to specify a single value of $\frac{pV}{T}$ for the gun region and the drift region and the correction factor for the anode lens must be $\sqrt{1.1}$. The arguments presented above indicate that

neglecting relativistic effects in the lens region will result in about a 10 percent error in the focal length of the lens. In the drift region it is possible to specify an equivalent perveance. If the value of p_{eq} and V_{eq} as defined for the drift region by Eqs. 4A, 5A, and 6A are used to compute $p \frac{V}{T}$, at 200 kv, $p = .125 \times 10^{-6}$, $\frac{V}{c} \approx 0.7$

$$p_{eq} = .086 \times 10^{-6}$$

$$V_{eq} = 255 \text{ kv}$$

and
$$\frac{p_{eq} V_{eq}}{T} = \frac{.086 \times 10^{-6} \times 2.55 \times 10^{-5}}{1100} = 19.9 \times 10^{-6}$$

This result is close to that estimated for the gun region and the value of $\frac{pV}{T}$ for all cases was chosen to be $\frac{p_{eq} V_{eq}}{T}$

The preceding arguments are quite qualitative but they do indicate that the relativistic corrections are small. Fortunately, the actual beam size does not change very rapidly with $\frac{pV}{T}$ for large values of $\frac{pV}{T}$ because thermal effects are relatively small. At lower values of $\frac{pV}{T}$, relativistic effects are not important and the calculations are correct.

DISTRIBUTION LIST

Copies

Aeronautical Systems Division Air Force Systems Command United States Air Force Wright-Patterson Air Force Base Dayton, Ohio ATTN: ASRNET-1, Contract AF 33(616)-8369	4 & 1 Reproducible
ASTIA (TISIA) Arlington Hall Station Arlington 12, Va.	20
Advisory Group on Electron Devices 346 Broadway, 8th Floor New York 13, New York ATTN: Mr. H. N. Serig	4
Air Force Cambridge Research Laboratories L. G. Hanscom Field Bedford, Mass. ATTN: CRRS, Mr. R. W. Wagner	1
Electronic Systems Division L. G. Hanscom Field Bedford, Mass. ATTN: ESRDE, Major J.W. Van Horn	1
Rome Air Development Center Griffiss Air Force Base New York ATTN: RALTP, Mr. H. Chiosa	1
Commanding Officer U. S. Naval Ordnance Laboratory Corona, California ATTN: Miss Virginia L. Parker	1

Distribution List (Continued)

Copies

Chief, Bureau of Ships Department of the Navy Washington 25, D. C. ATTN: Mr. H. J. Riegger	1
Chief, Bureau of Ships Department of the Navy Washington 25, D. C. ATTN: Mr. Charles Walker	1
Commanding Officer USASRDL Fort Monmouth, New Jersey ATTN: Mr. Harold J. Hersh, SIGRA/SL-PRM	1
Commanding Officer USASRDL Fort Monmouth, New Jersey ATTN: Mr. Irving Reingold, Microwave Tubes Branch	1
Commanding Officer Diamond Ordnance Fuze Laboratories Microwave Tube Branch Washington 25, D. C.	1
General Electric Wave Tube Product Section 601 California Avenue Palo Alto, California ATTN: Technical Library	1
Hughes Research Laboratories Malibu, California ATTN: Dr. M. Currie	1
Litton Industries, Incorporated 960 Industrial Road San Carlos, California ATTN: Dr. J. Hull	1

Distribution List (Continued)

Copies

Raytheon Corporation Waltham, Massachusetts ATTN: Dr. P. Derby	1
Bendix Corporation Research Laboratories North Western Highway & 10 1/2 Mile Road Southfield, Michigan ATTN. Mr. A. G. Peifer	1
Radio Corporation of America 415 South Fifth Street Harrison, New Jersey ATTN. Mr. H. K. Jenny 55-2	1
Sperry Gyroscope Company Great Neck New York ATTN: Dr. L. W. Holmboe	1
Aerospace Corporation 2400 E. El Segundo Boulevard El Segundo, California ATTN. Mr. B. J. DuWaldt	1
Director U. S. Naval Research Laboratory Washington 25, D. C. ATTN Code 5240	1
Director U. S. Naval Research Laboratory Washington 25, D. C. ATTN: Code 5244, Mr. H. D. Arnett	1